

Introduction to Computational Medicine I: Computational Anatomy (BME 580.432)

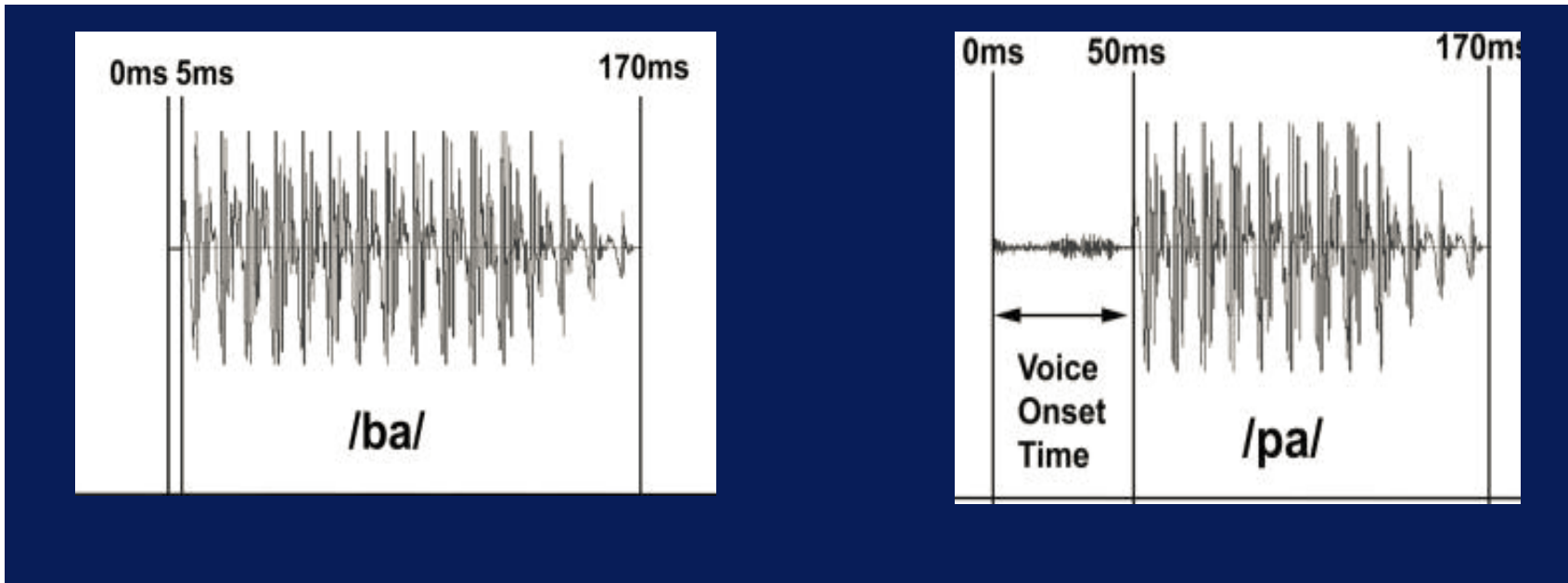
Michael I. Miller

Tilak Ratnanather

Daniel Tward



Temporal shifting and scaling has been the organizing principle of communications for 100 years.



Temporal Signals: time–shift–scale
 $t \in \mathbb{R}$ $\phi: X(t) \mapsto A(t) \cdot X(t + t_d + s(t))$

Amplitude Modulator	Carrier	Time-Shift Linear Phase	Frequency Modulation
---------------------	---------	-------------------------	----------------------

Temporal shifting and scaling has organized the information in communications.

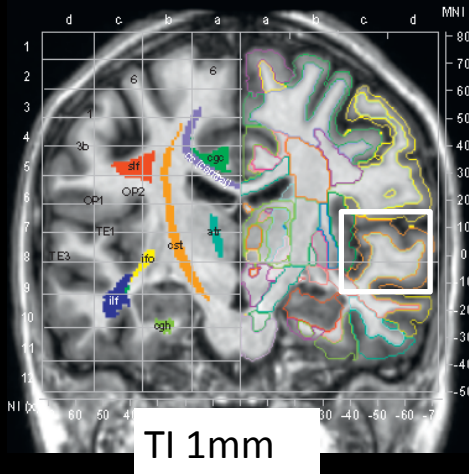
The rotations-translations-shifts-scales (matrix groups) and vector fields are the coordinate system transformations which play the role of for medical images.

The Model of Medical Images

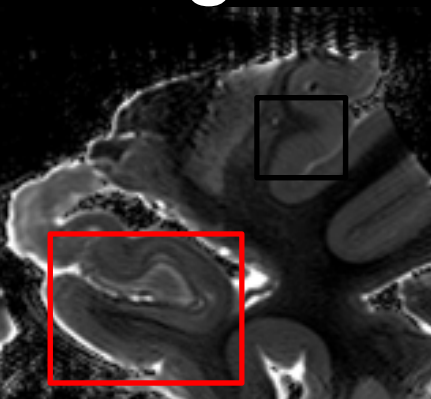
Images: space–shift–scale – translate
 $x \in \mathbb{R}^3 \quad \phi: I \mapsto I(x + Ax + v(x))$

Image	Space	Matrix Group	Vector
		Translate	Field
		Rotate	
		Scale	

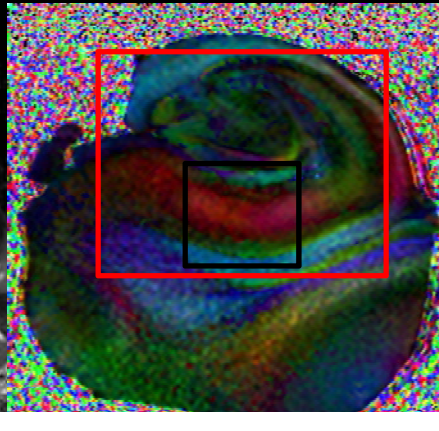
Medical Images & Neuroinformatics



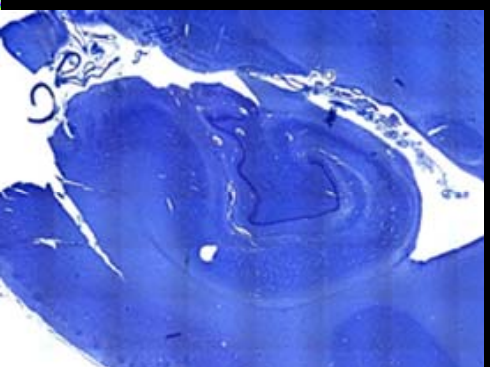
T1 1mm



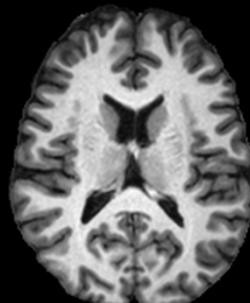
T1 High Field 11.7T 200 μ



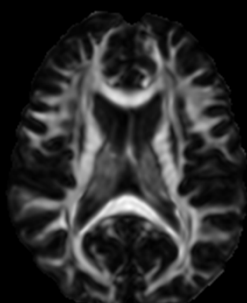
DTI High Field 11.7T



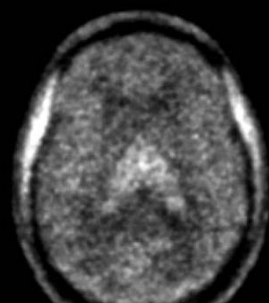
Histology μ



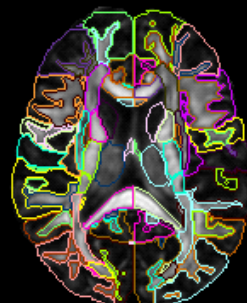
T1



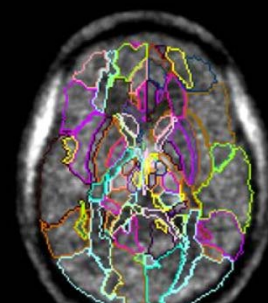
FA



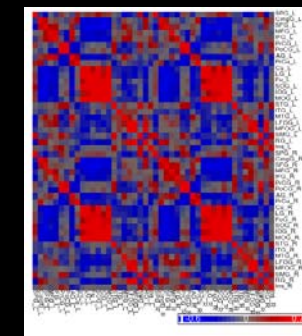
PET



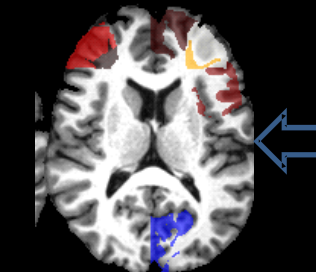
Choline



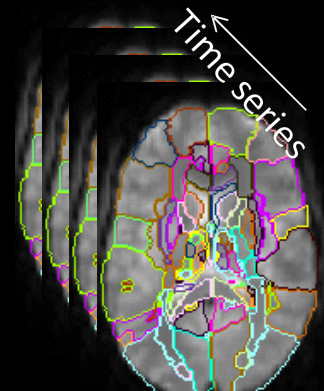
Creatine



RS-functional
connectivity



5



Time series

Notation: Coordinates and Images

Spatial Coordinates and Vector Notation

$$x \doteq (x_1, x_2) \in X \subset \mathbb{R}^2$$

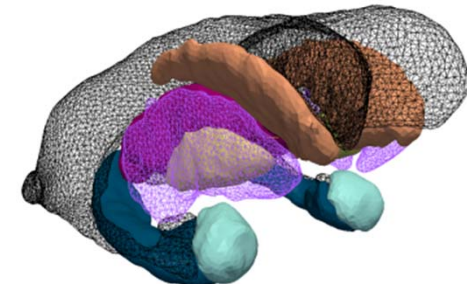
$$x \doteq (x_1, x_2, x_3) \in X \subset \mathbb{R}^3$$

Pointset Images (Landmarks): $I \equiv \{x_i, i = 1, 2, \dots, n\}$

Scalar Images: $I \equiv I(x), x \in X \subset \mathbb{R}^3$

$$I: x \in X \mapsto I(x) \in [0, 255]$$

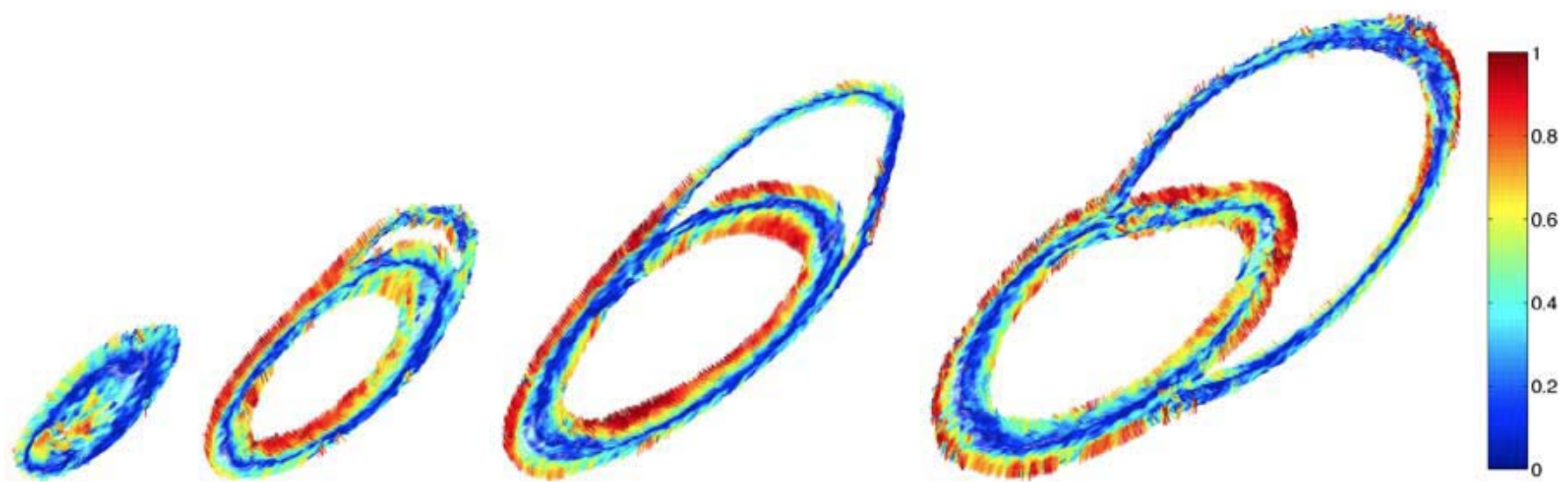
Vector Images



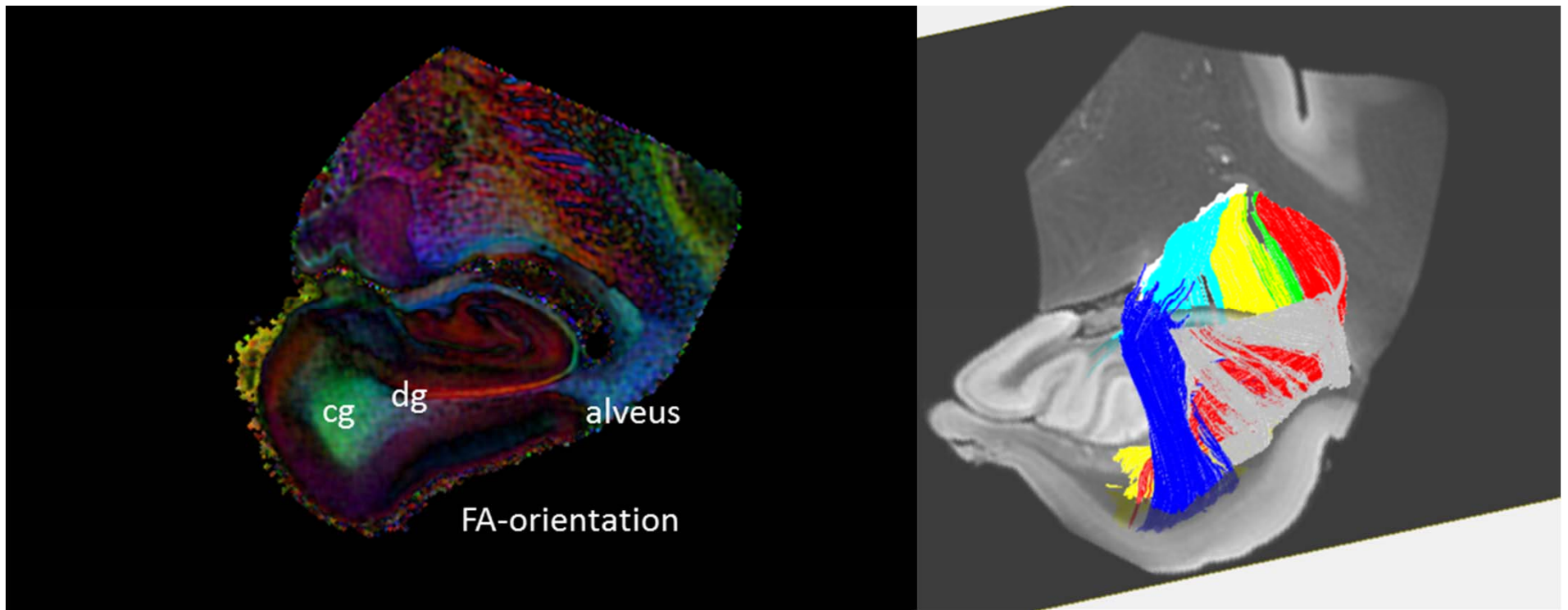
Matrix Images (DTI)

Cardiac Fibers

(color coded as dot product of vectors)



White Matter Trajectories



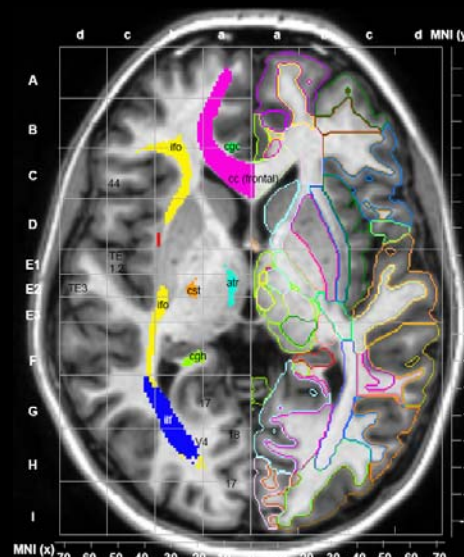
Red: lateral ↔ medial;
Green: anterior ↔ posterior;
Blue: inferior ↔ superior

High Throughput Neuroinformatics

www.MRICloud.org

THE BRAIN HAS 100'S OF REGIONS

Superior parietal gyrus
Superior frontal gyrus
Middle frontal gyrus
Inferior frontal gyrus
Precentral gyrus
Postcentral gyrus
Angular gyrus
Pre-cuneus gyrus
Cuneus gyrus
Lingual gyrus

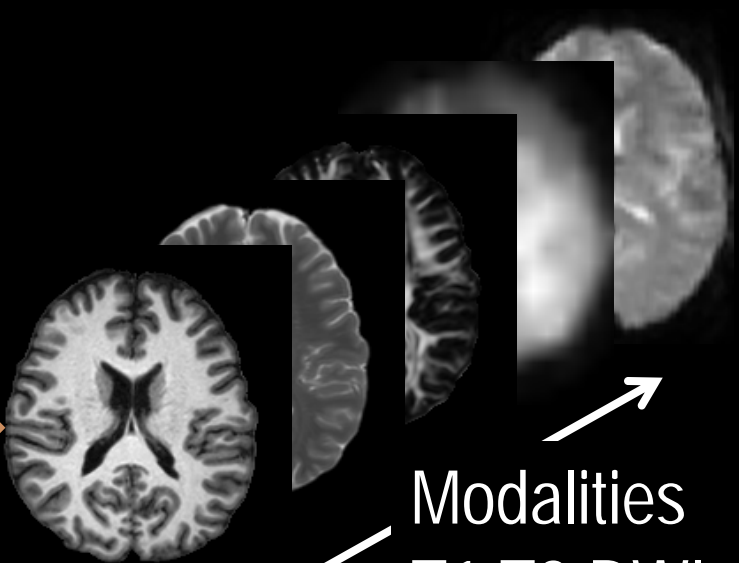


Atlas

Amygdala
Caudate
Globus Pallidum
Hippocampus
Putamen
Thalamus
Red Nucleus
Substantia Nigra
Hypothalamus
Nucleus Accumbens
Dentate Gyrus

Corticospinal tract
Internal capsule
Thalamic radiation
Corona radiata
Fornix
Superior longitudinal fasciculus
Inferior front-occipital fasciculus
Corpus Callosum
External capsule
Uncinate fasciculus

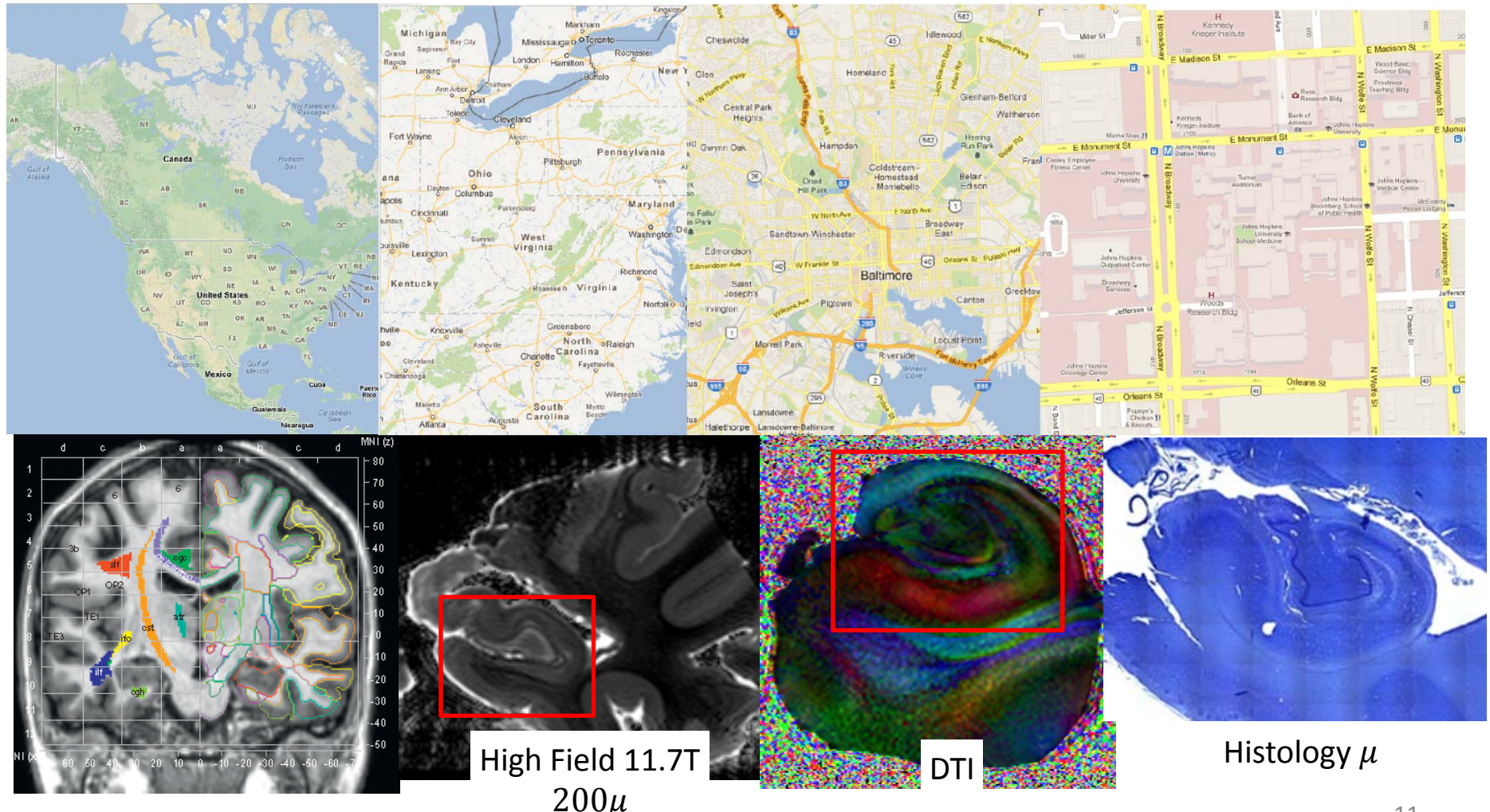
GPS
POSITIONING
SYSTEM



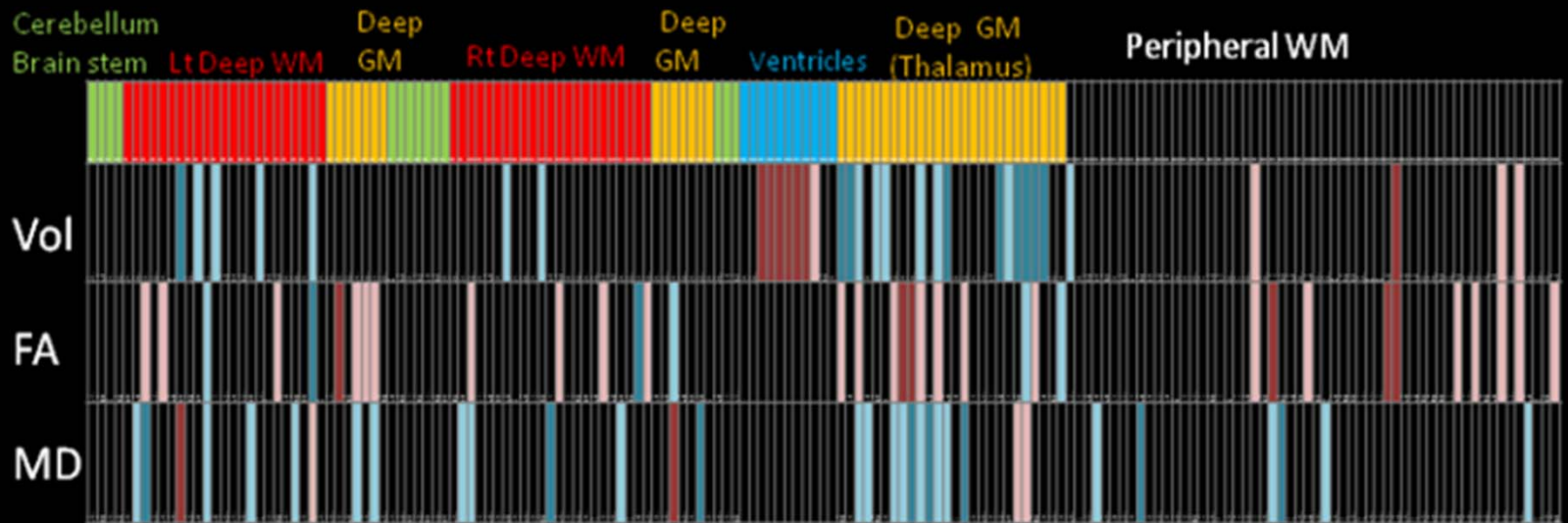
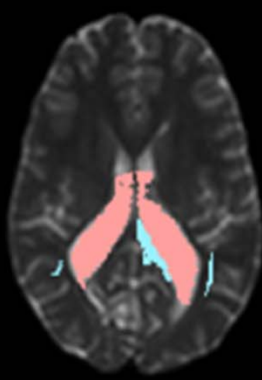
Modalities
T1, T2, DWI,
PET, fMRI



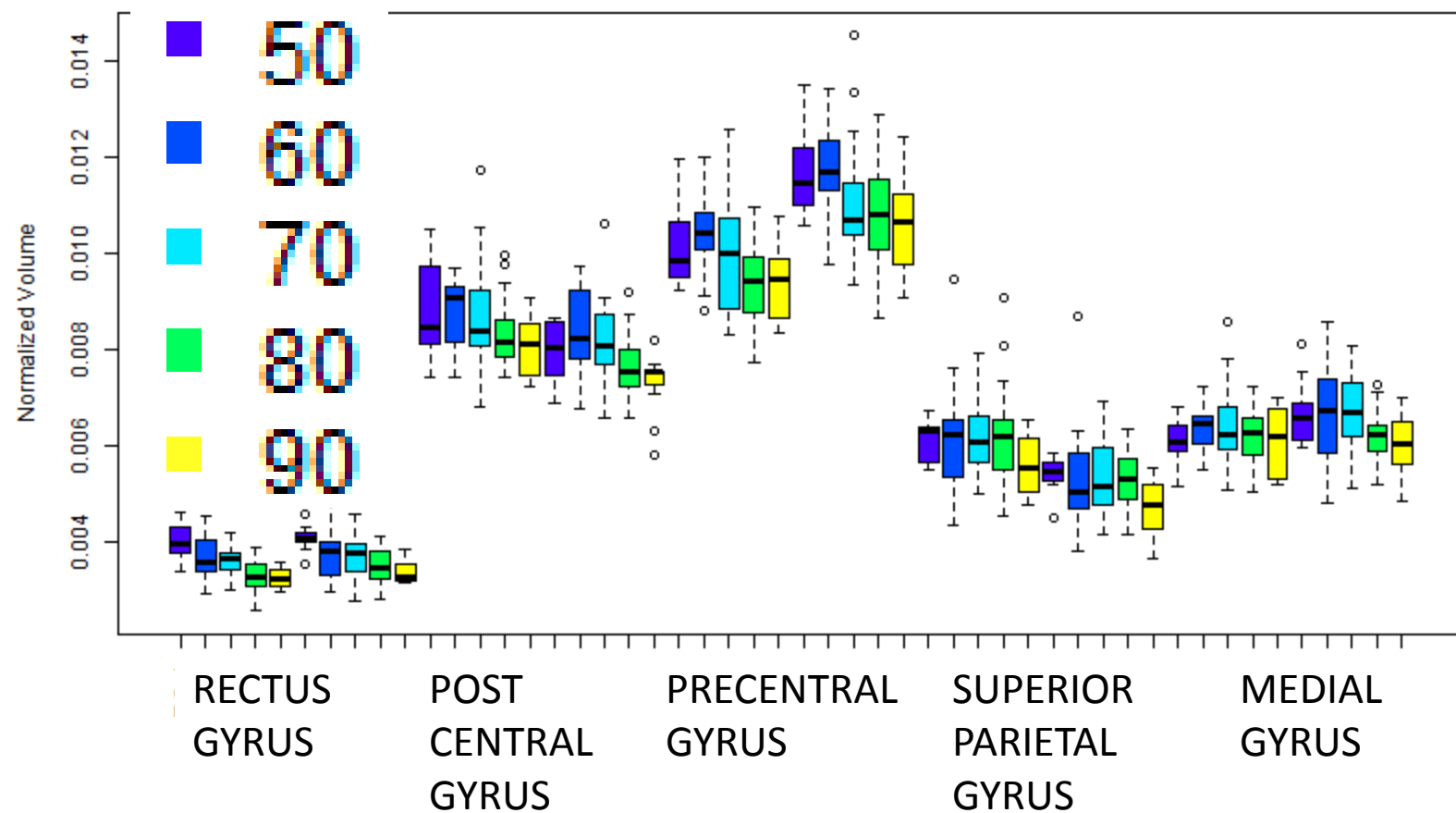
GPS positions information across scales using coordinate system transformations. These are called diffeomorphisms: structure preserving mappings.



BRAINS BECOME 1000 BYTE INDEX



T1 Gray matter: Aging



Gray matter spaces are decreasing!

These statistics form
the basis for
Personalized
Radiomics
for Health Care.

The High-Throughput
Pipeline is a Medical
Image Analysis,
Artificial Intelligence,
Software as a Service

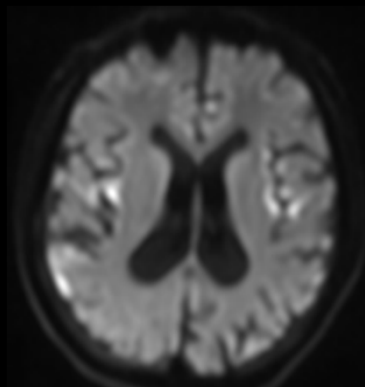
www.MRICloud.org

Ask Watson

Ask Watson

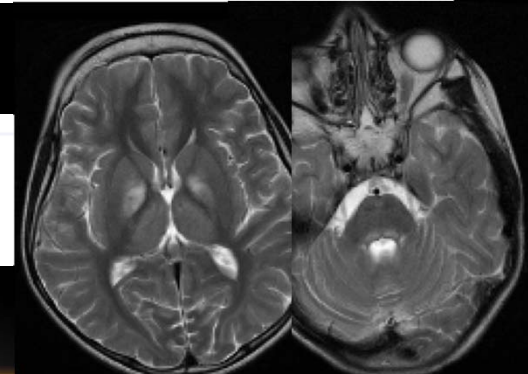
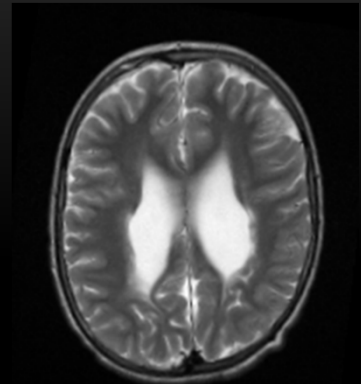
COLLECT MANY TEXT RECORDS FROM
DATA BASE

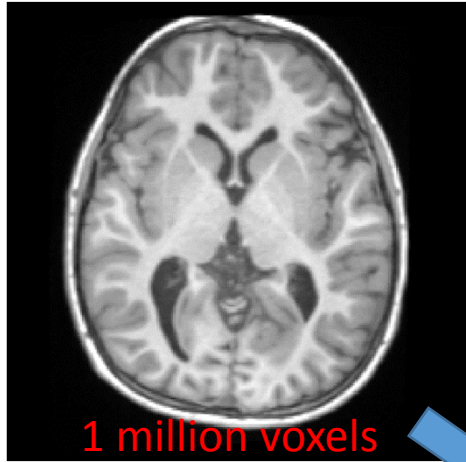
the presence of T2/FLAIR hyperintensity in the periventricular white matter, most prominently in the regions where ventricular dilatation is most pronounced, and the presence of parieto-occipital white matter volume loss



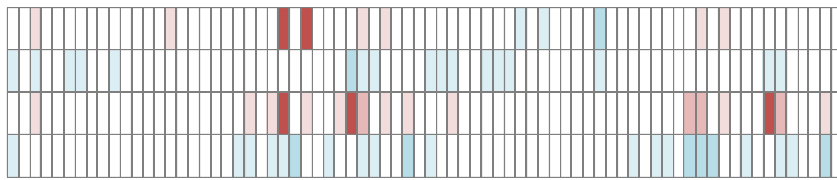
Interval progression of disease, with multifocal areas of acute to early subacute infarction involving the cortex and subcortical white matter, Moderate parenchymal volume loss involving the supratentorial and infratentorial brain

stable T2/FLAIR hyperintense signal within the central gray matter as well as brain stem and cerebellum as detailed above consistent with mitochondrial disease





1000 byte vector



Language generation

Severe bi-hemispheric atrophy. Severe frontal lobe atrophy. Temporal lobe and occipital lobe are preserved. Severe ventricle expansion in the anterior horn of the lateral ventricles and the body of the lateral ventricles.

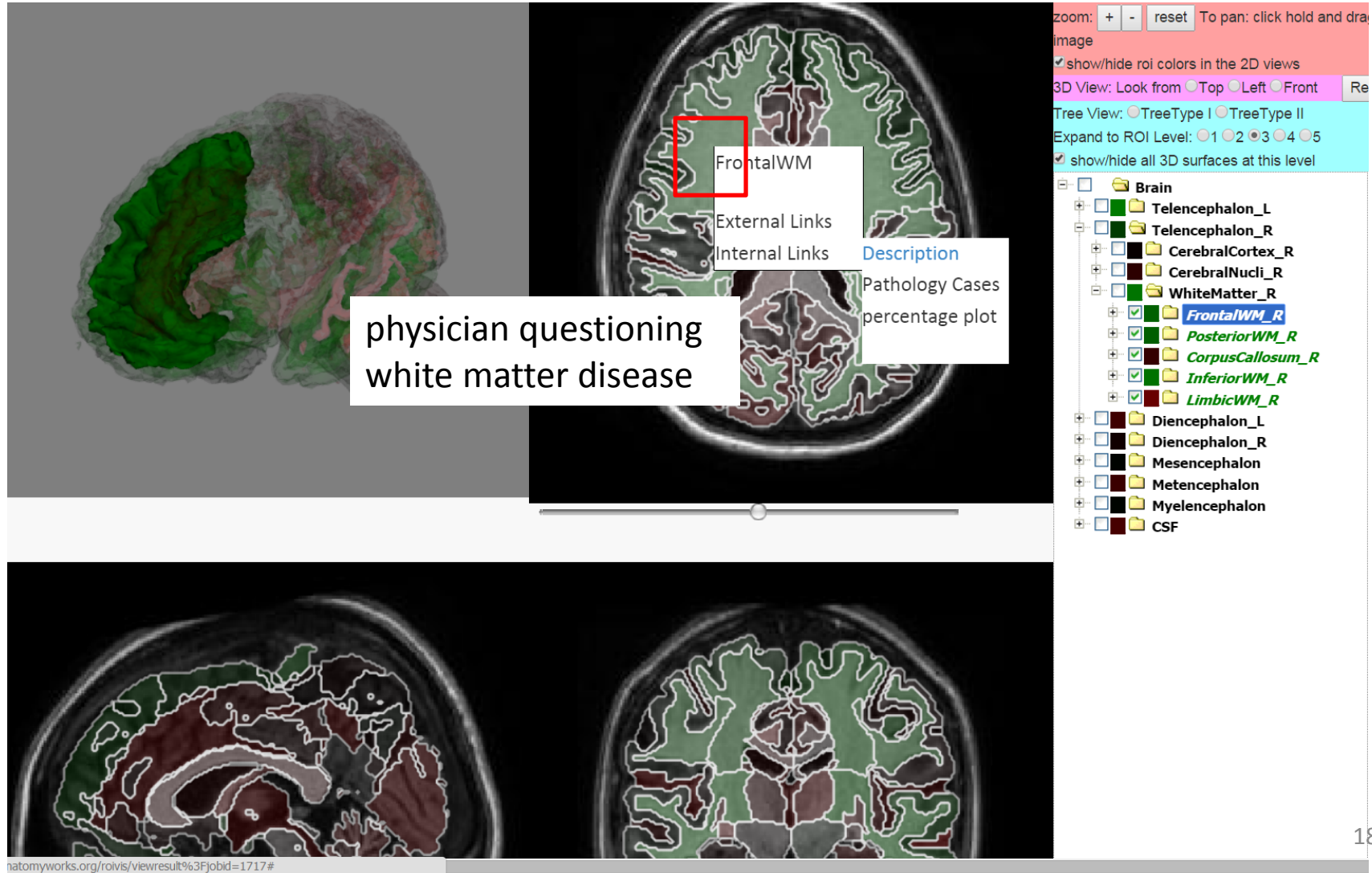
WATSON SAYS

Clinical filter

Tissue Atrophy				
Cerebrum (neo cortex areas)	Hemisphere	Left		-4.00
		Right		-3.34
frontal lobe L/R		Left	Type2 Level3'	-3.34
		Right		-3.17
parietal lobe L/R		Left	Type2 Level3'	-2.88
		Right		-1.87
temporal lobe L/R		Left	Type2 Level3'	2.67
		Right		2.65
occipital lobe L/R		Left	Type2 Level3'	0.90
		Right		1.32
insula L/R		Left	Type2 Level3'	-1.11
		Right		-0.56
inferior deep white matter L/R		Left	Type2 Level3'	-2.79
		Right		-1.43
posterior deep white matter L/R		Left	Type2 Level3'	-3.70
		Right		-2.72
Cerebrum (limbic) L/R	limbic (cingulate) L/R	Left	Type1 Level4	-2.69
		Right		-2.61
	limbic (hippocampus) L/R	Left	Type1 Level4	-0.16
		Right		-1.73
	limbic (medial temporal) L/R	Left	Type1 Level5	1.44
		Right		-0.57
	limbic (amygdala) L/R	Left	Type1 Level4	-1.26
		Right		-0.23
basal ganglia L/R	basal ganglia (caudate nucleus) L/R	Left	Type1 Level4	2.05
		Right		2.24
	basal ganglia (putamen) L/R	Left	Type1 Level4	-2.42
		Right		-3.33
	basal ganglia (globus pallidus) L/R	Left	Type1 Level4	-1.95
		Right		-2.01
thalamus L/R	thalamus L/R	Left	Type1 Level3	-2.73
		Right		-3.47
corpus callosum	corpus callosum	Left	Type1 Level3	-0.40
		Right		0.04
cerebellum	cerebellum		Type1 Level3	-0.12
midbrain	midbrain (tectum + tegmentum)	Left	Type1 Level5	-2.82
		Right		-2.52
pons	pons	Left	Type1 Level5	-1.81
		Right		-1.47
Expansion				
lateral ventricle L/R	anterior horn of lateral ventricle L/R	Left	Type1 Level5	5.15
		Right		5.03
	body of lateral ventricle L/R	Left	Type1 Level5	3.95
		Right		4.21
	posterior horn of lateral ventricle L/R	Left	Type1 Level5	1.19
		Right		2.63
3rd ventricle	3rd ventricle		Type1 Level5	2.70

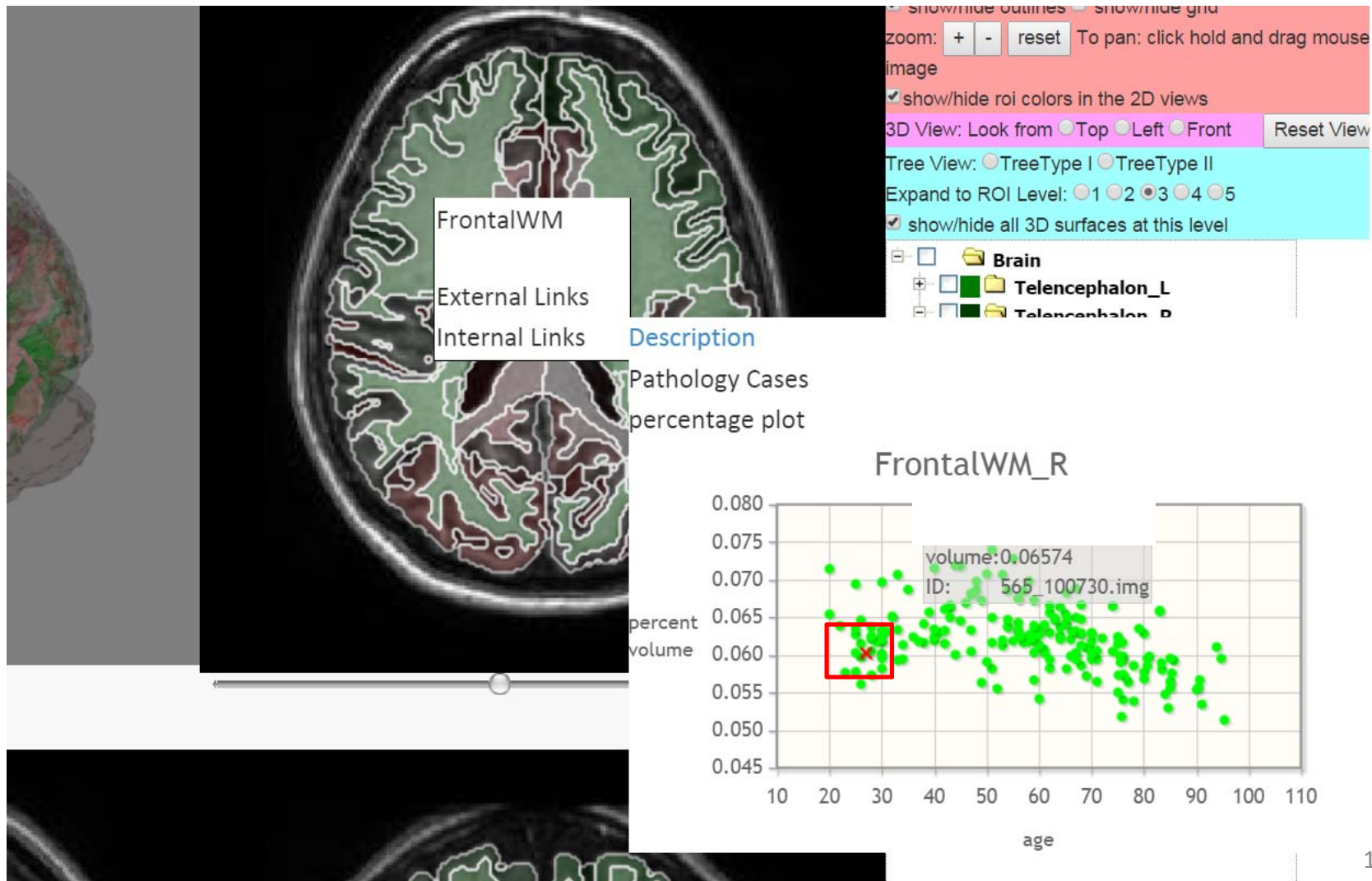
www.MRICloud.org

Patient Specific



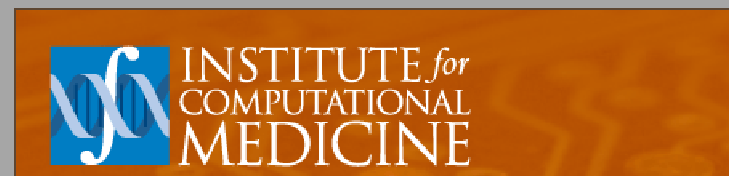
www.MRICloud.org

Patient Specific

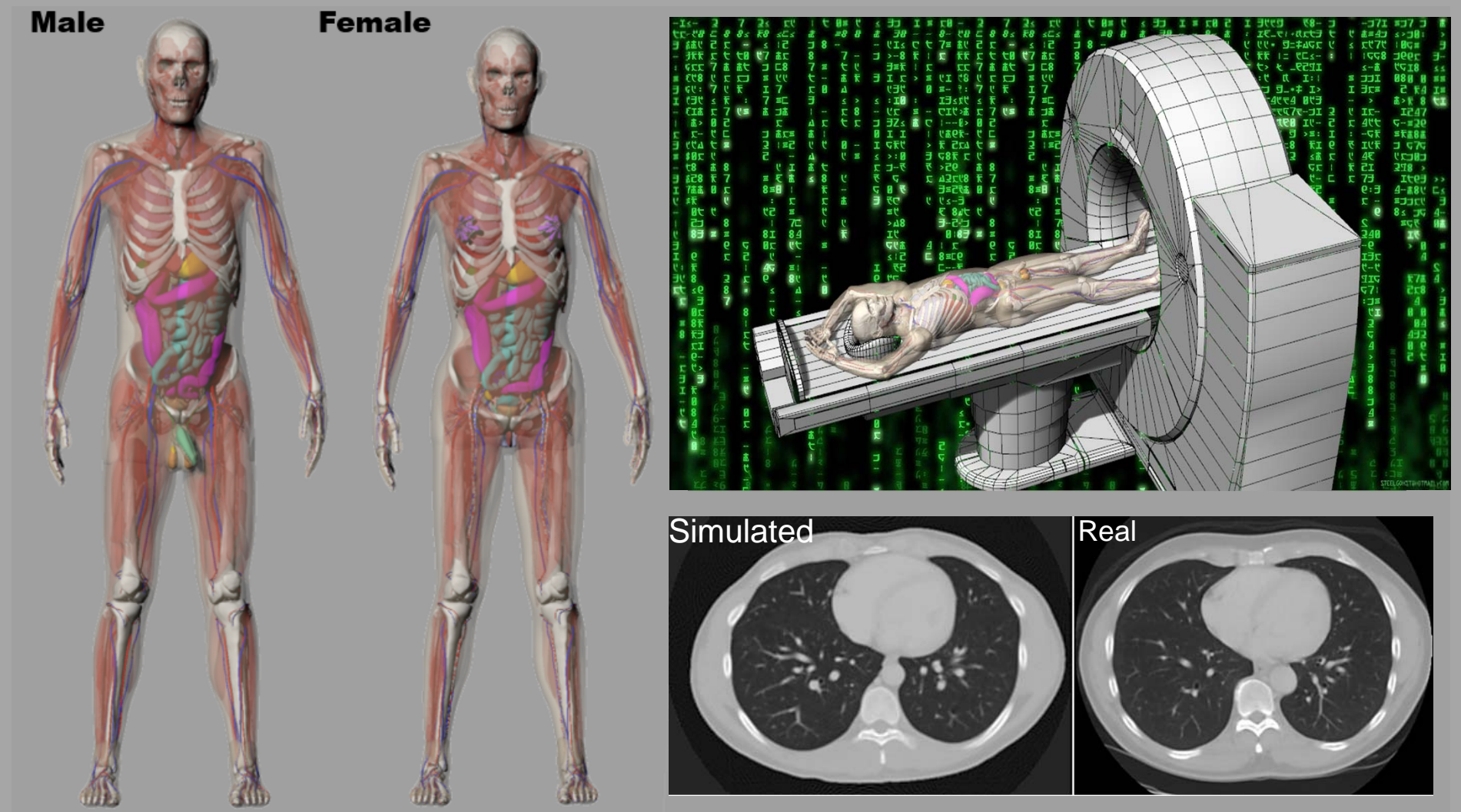


Whole Body Mapping

- W. Paul Segars, Ph.D. (Duke University)
- Michael I. Miller, Ph.D. (JHU)
- Daniel J. Tward (JHU)
- J. Tilak Ratnanather, D.Phil. (JHU)



4D eXtended CArdiac-Torso (XCAT) Phantoms

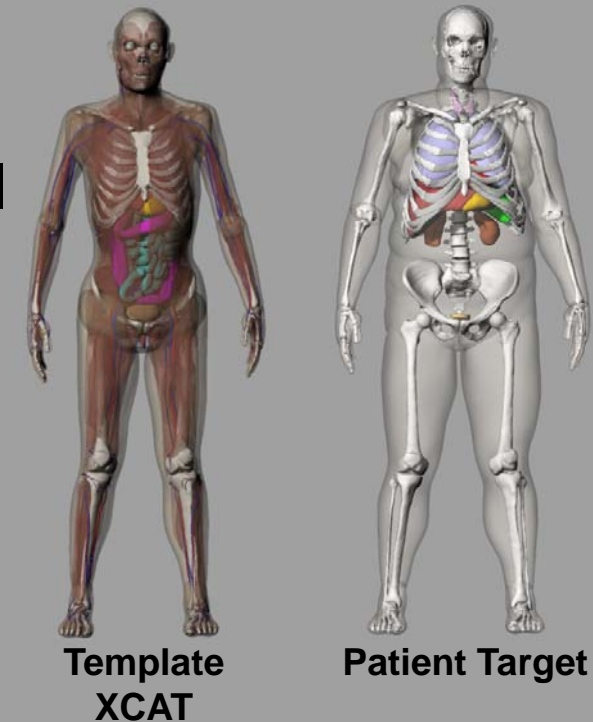
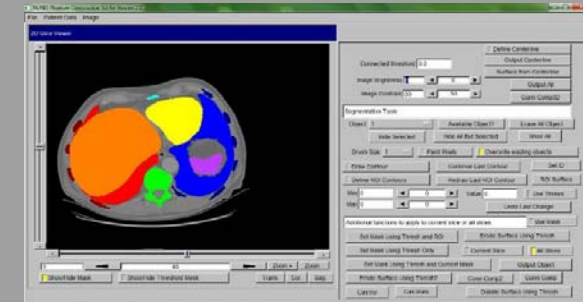


Based on Segmented Human Imaging Data, Detailed Anatomy defined with Spline Surfaces

Combined with algorithms that mimic modern imaging devices, can produce realistic imaging data

Phantom Construction

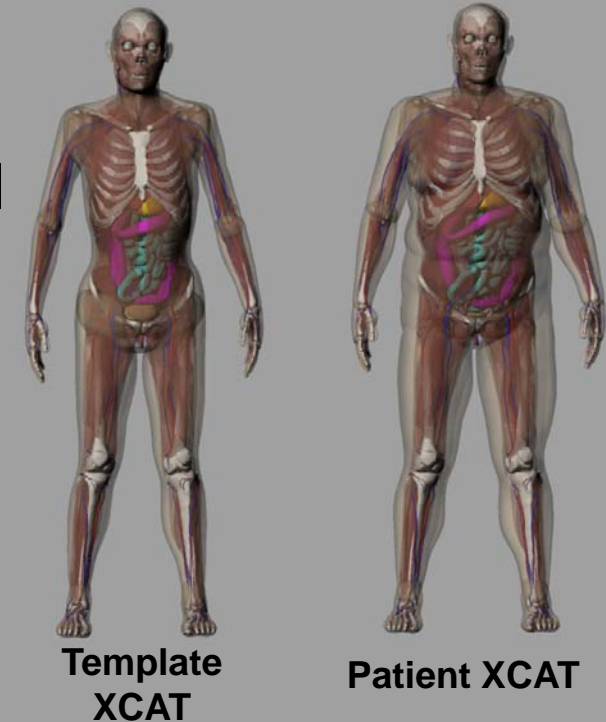
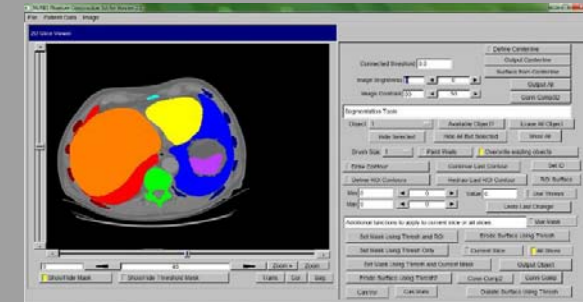
- Segment patient CT data (bones and major organs) to create an initial model
 - Fit arms/legs to patient model using XCAT models scaled to patient size
- Utilize MC-LDDMM mapping algorithm to morph one complete template XCAT phantom (including cardiac & respiratory motions) to the target model
 - Defines unsegmented structures (vessels, muscles, tendons, ligaments)
 - No need to segment all structures
- Using this technique, a phantom can now be completed in days instead of months



Tward et al., Patient Specific Dosimetry Phantoms Using Multichannel LDDMM of the Whole Body, International Journal of Biomedical Imaging, vol. 2011, Article 481064

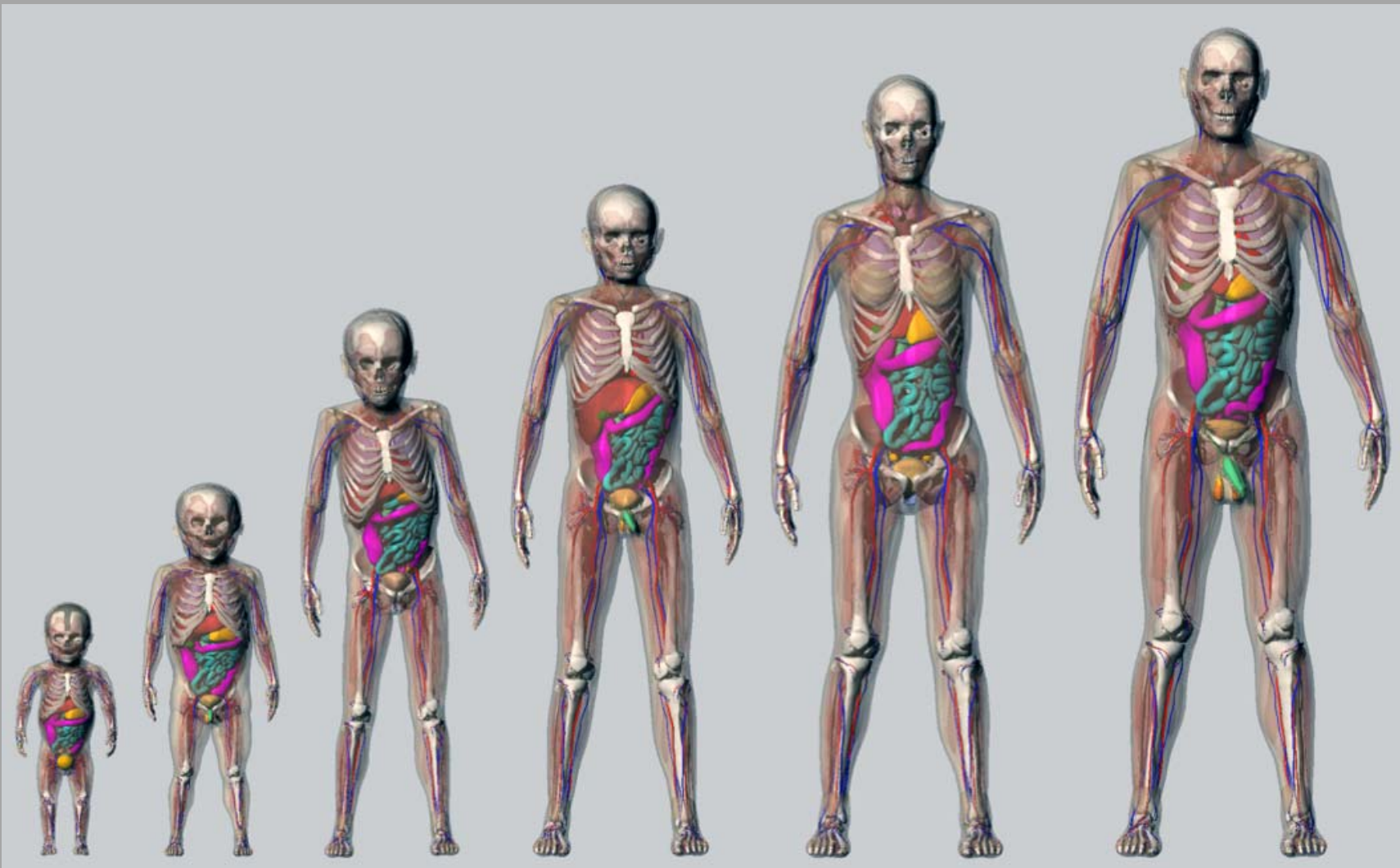
Phantom Construction

- Segment patient CT data (bones and major organs) to create an initial model
 - Fit arms/legs to patient model using XCAT models scaled to patient size
- Utilize MC-LDDMM mapping algorithm to morph one complete template XCAT phantom (including cardiac & respiratory motions) to the target model
 - Defines unsegmented structures (vessels, muscles, tendons, ligaments)
 - No need to segment all structures
- Using this technique, a phantom can now be completed in days instead of months



Tward et al., Patient Specific Dosimetry Phantoms Using Multichannel LDDMM of the Whole Body, International Journal of Biomedical Imaging, vol. 2011, Article 481064

New XCAT Phantoms

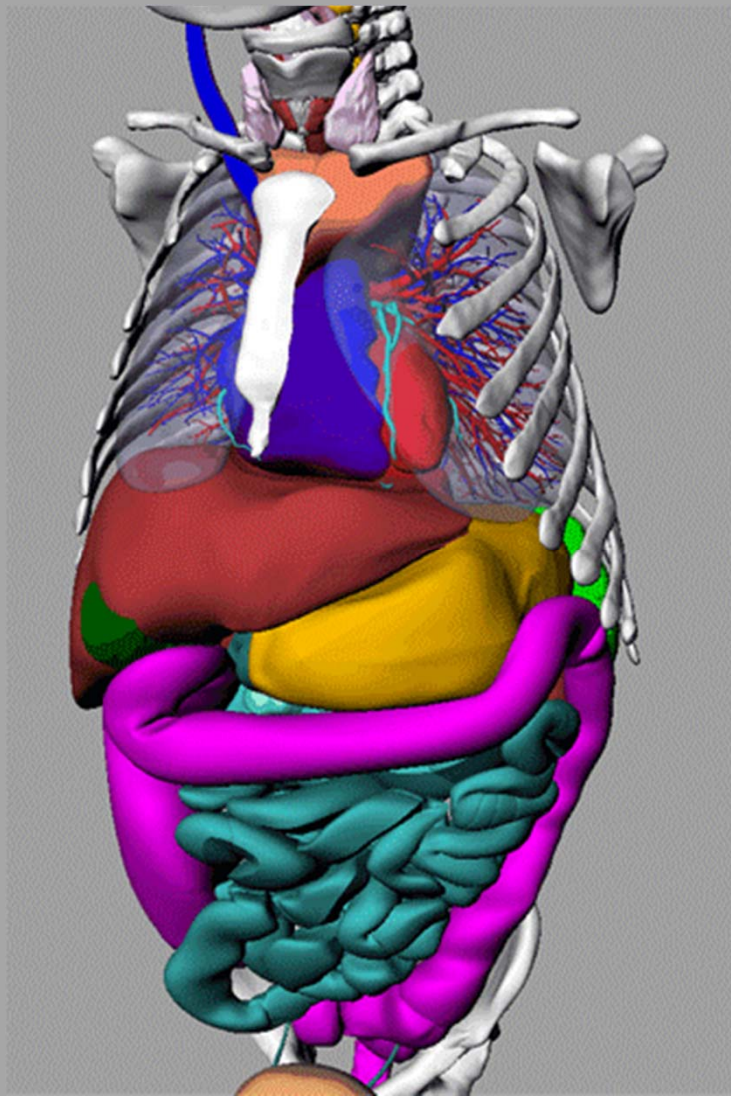


Segars et al., Population of anatomically variable 4D XCAT adult phantoms for imaging research and optimization, *Med Phys*, 40, (2013).

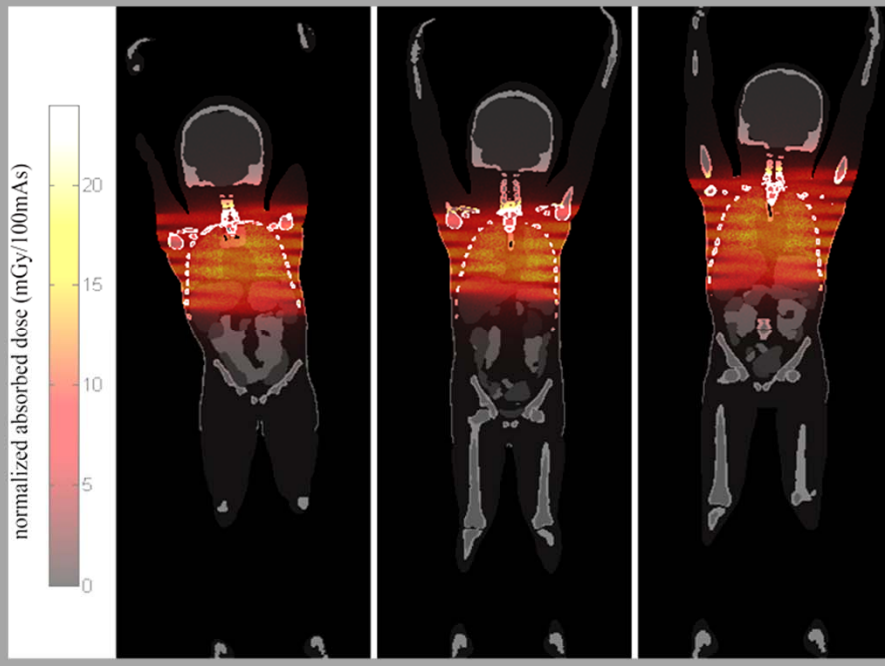
Norris et al., A set of 4D Pediatric XCAT Reference Phantoms for Multimodality Research, *Med Phys*, 41, (2014).

Segars et al., The development of a population of 4D pediatric XCAT phantoms for imaging research and optimization, *Med Phys*, (2015).

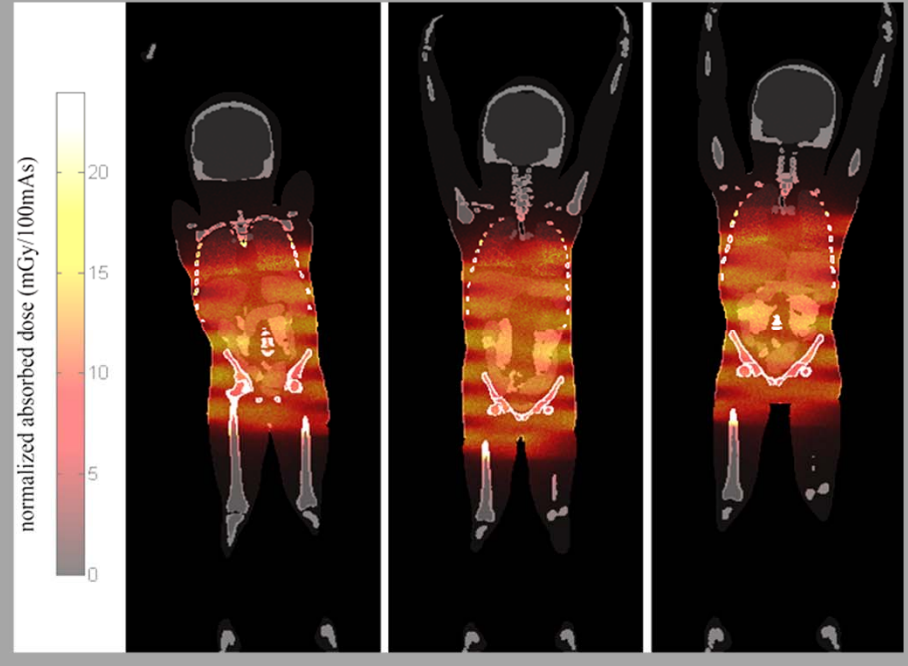
Diffeomorphisms from template carry fine details to the target



Accurate Dose Estimation from Imaging Protocols



Chest Scan

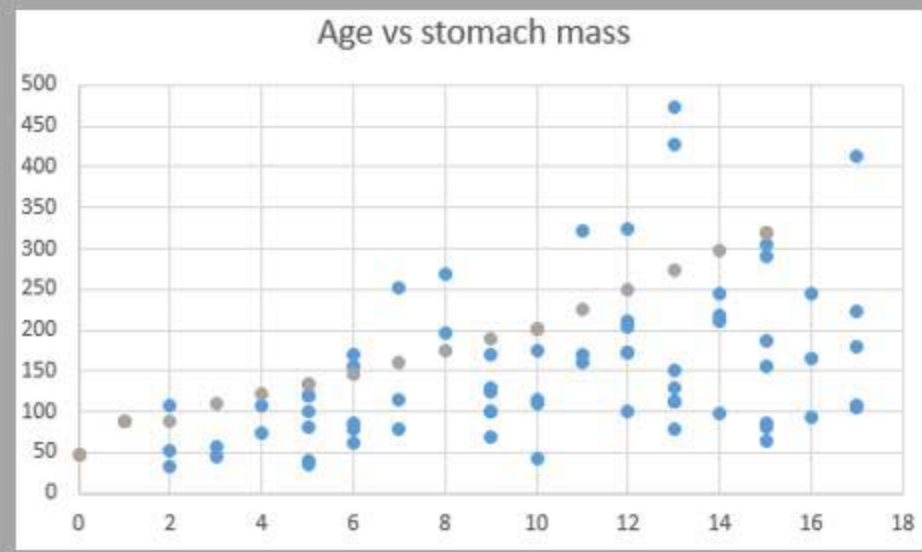
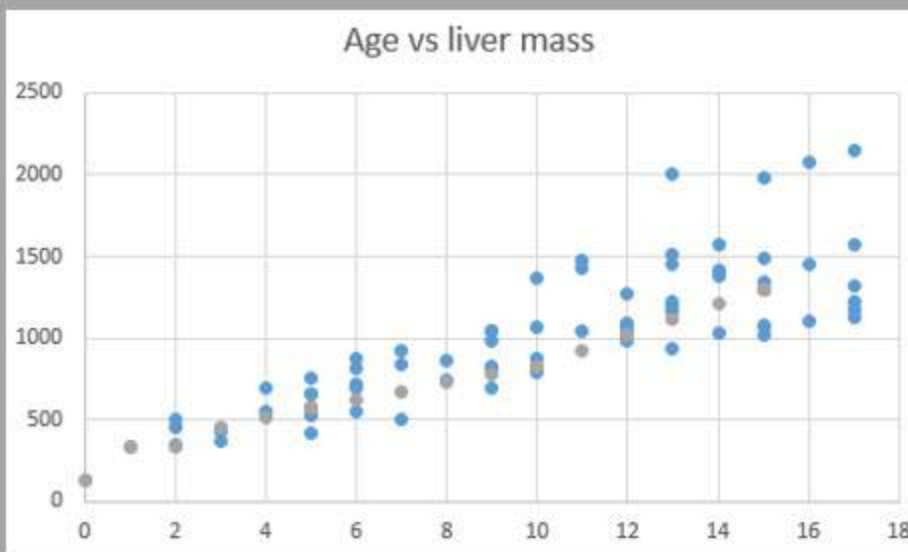
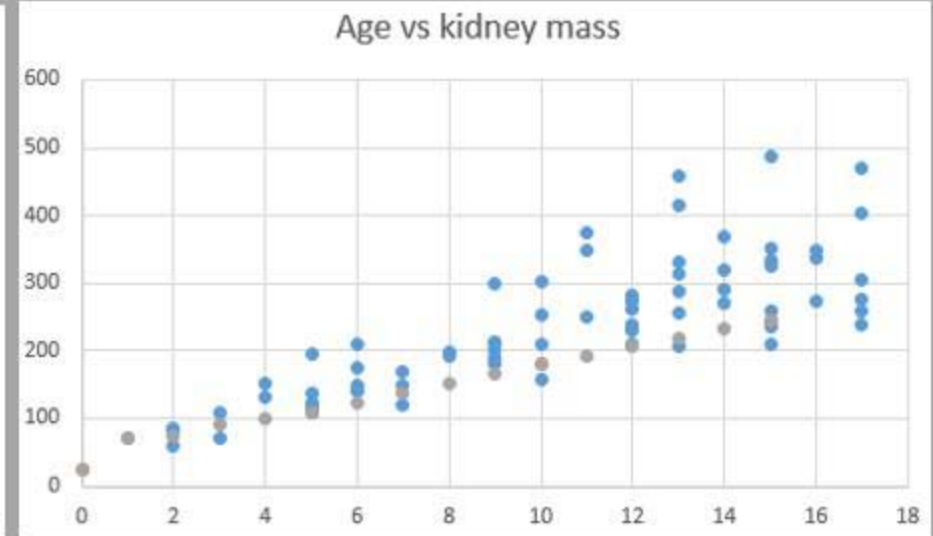
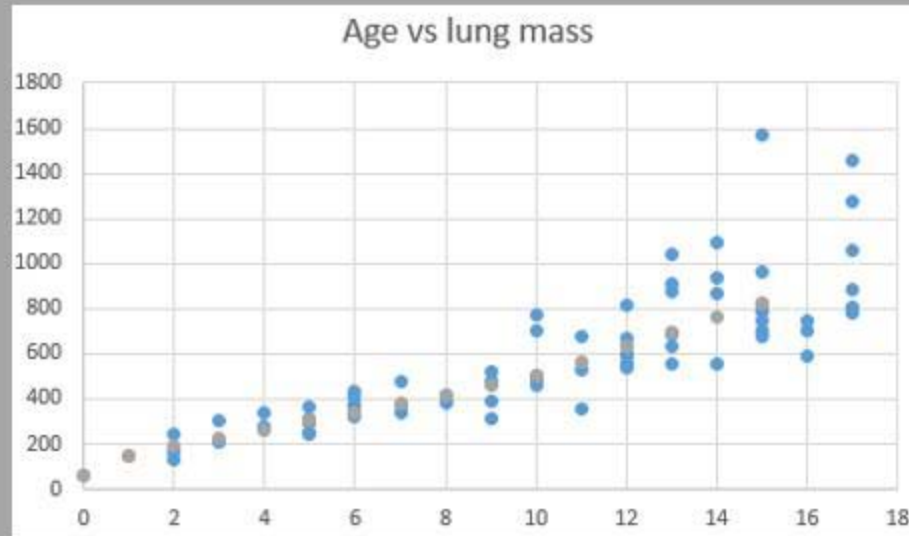


Abdomen Scan

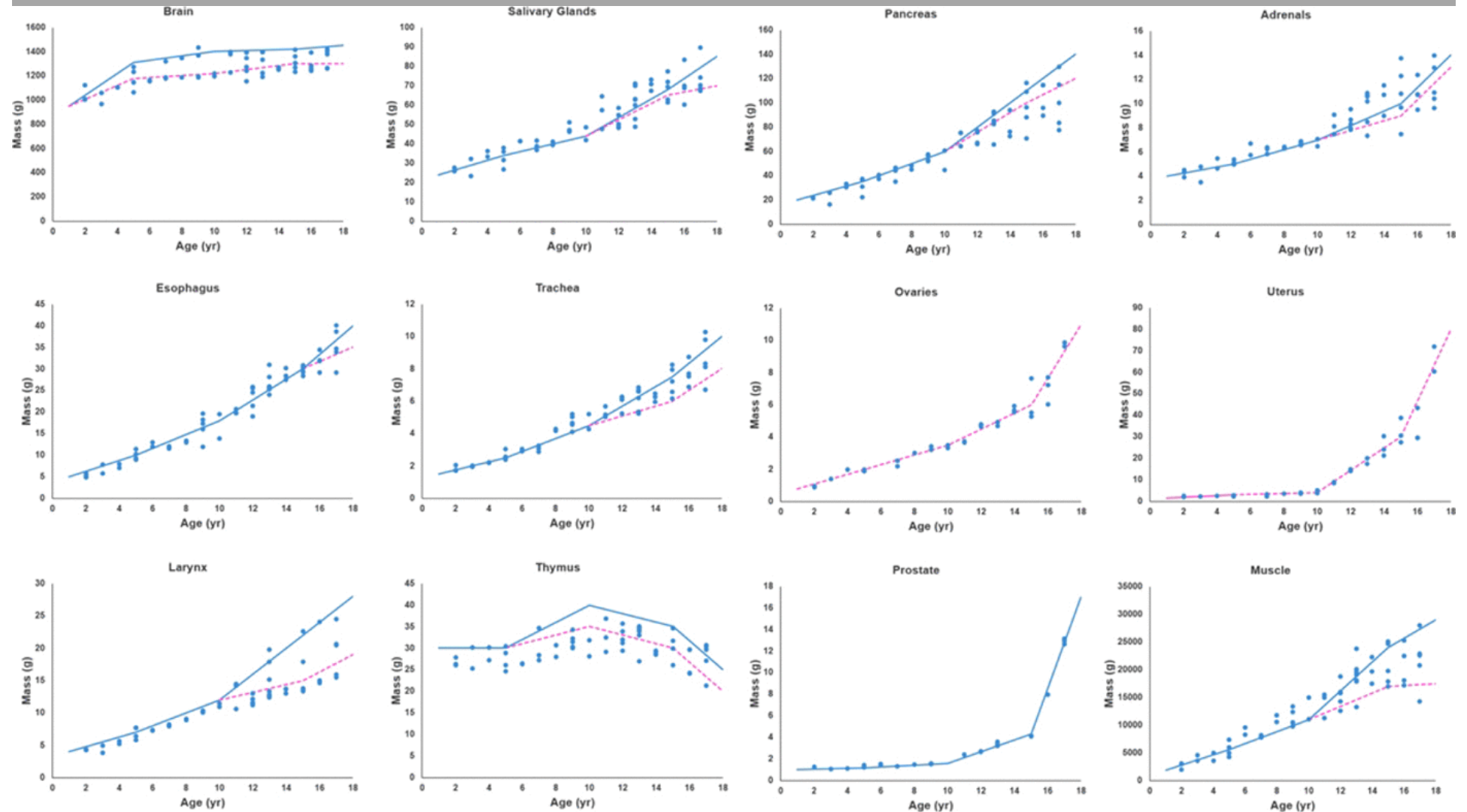
Coronal dose estimation in three 2 year-old phantoms for chest and abdomen CT imaging protocols

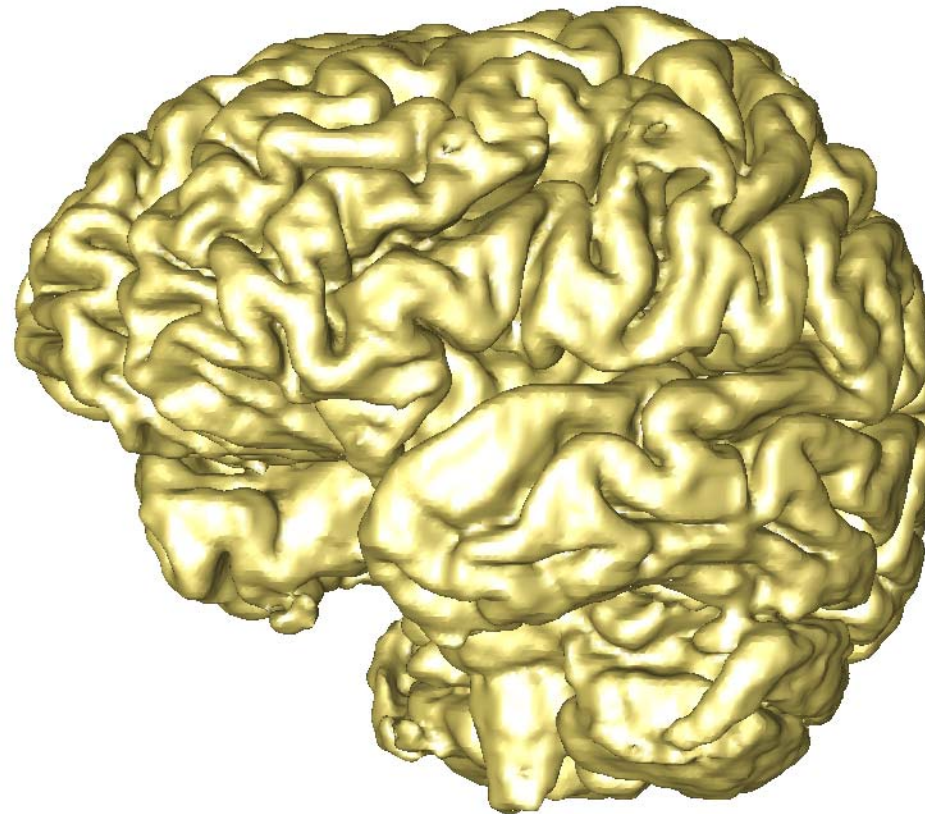
Brief Review: Norris et al. (2014) Proc. of SPIE Vol. 9033, 90331V
Experiments: Li et al. (2011) Med Phys. 38: 397-407 and 408-419

Calculated organ masses for selected organs vs. linearly interpolated ICRP values

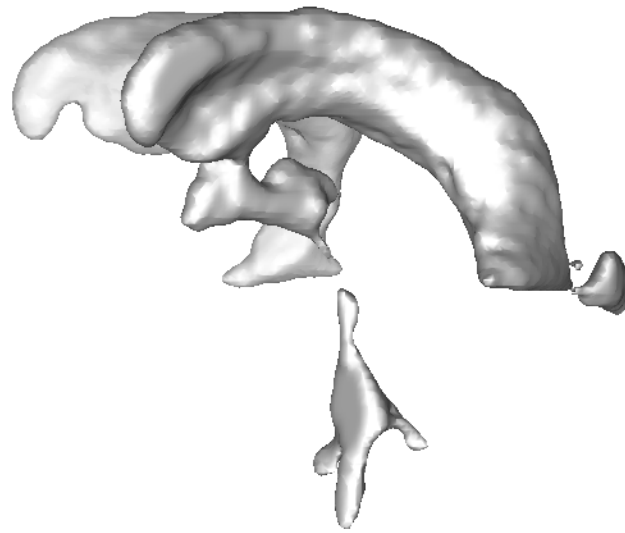


Mass versus age for the organs and structures predicted by the MC-LDDMM transform

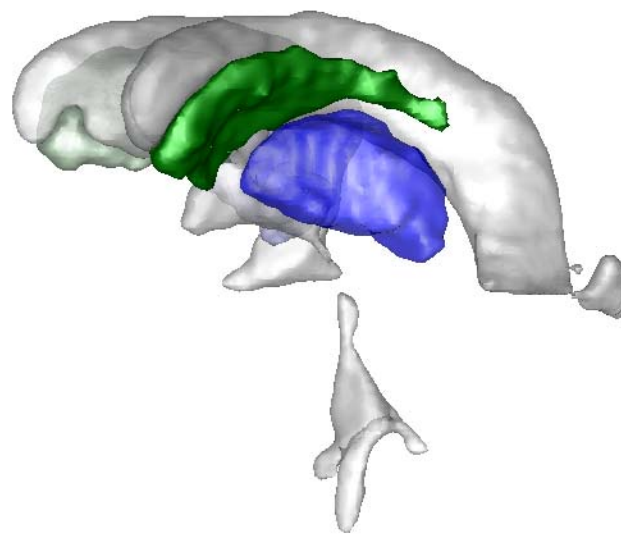




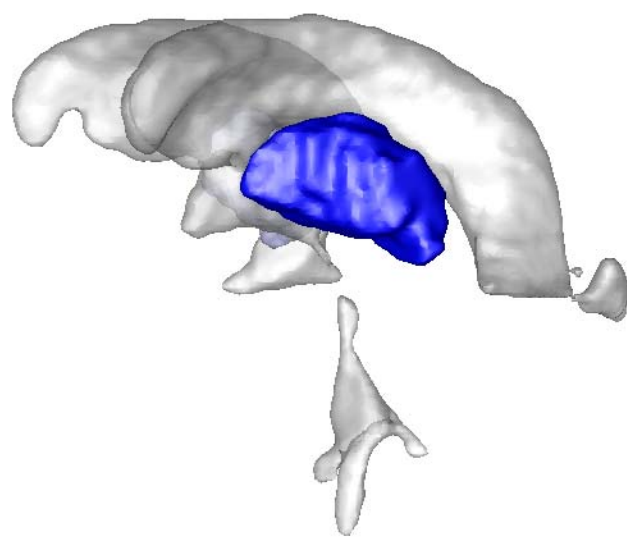
Cortex - right side



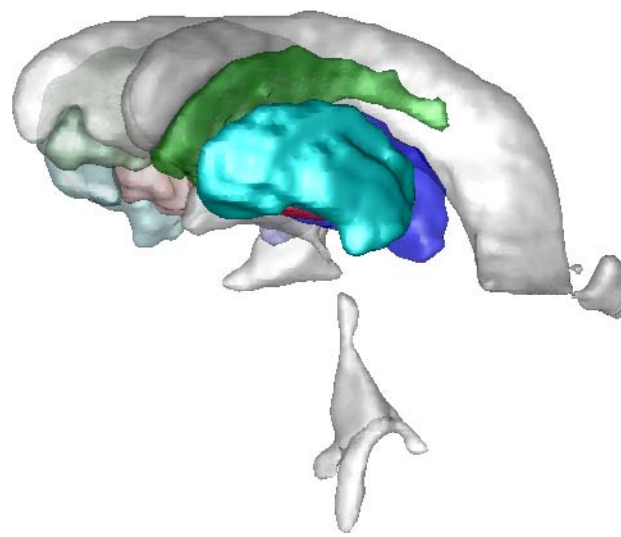
Corpus callosum
& midbrain



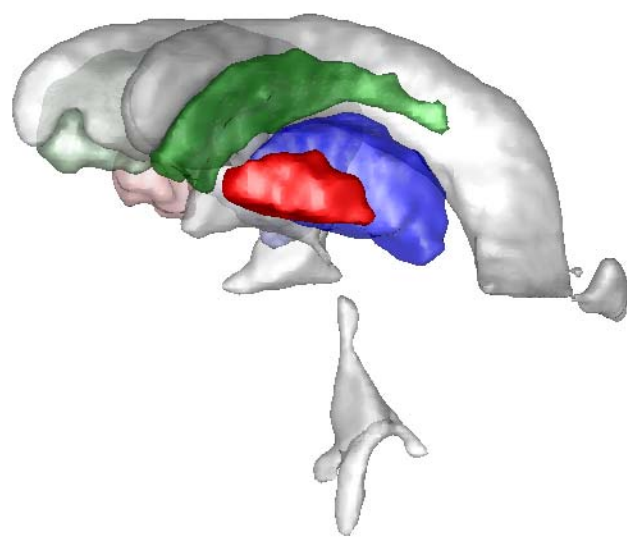
Caudate (green) &
Thalamus (blue)



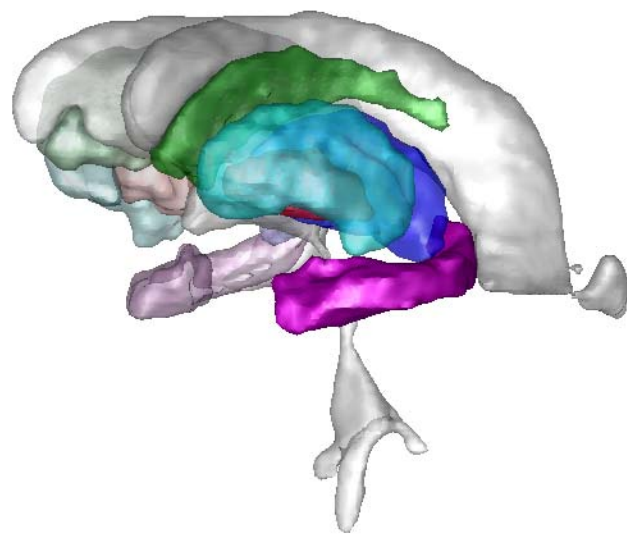
Thalamus (blue)



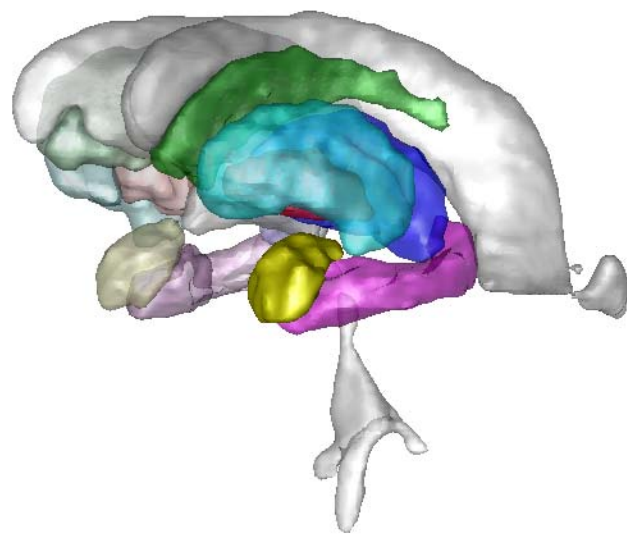
putamen (light blue)



Globus pallidus (red)



Hippocampus (purple)



Amygdala (yellow)

